Linear instability of a coflowing jet under an axial electric field

Fang Li, Xie-Yuan Yin, and Xie-Zhen Yin*
Department of Modern Mechanics, University of Science and Technology of China, Hefei, Anhui 230027, People's Republic of China
(Received 25 April 2006; revised manuscript received 30 June 2006; published 18 September 2006)

A temporal linear stability analysis is carried out for a coflowing jet with two immiscible inviscid liquids under a uniform axial electric field. According to the electrical properties of the inner and outer liquids, four cases, i.e., IDOC (inner: dielectric; outer: conductor), ICOD (inner: conductor; outer: dielectric), ICOC (inner and outer: conductor), and IDOD (inner and outer: dielectric), are considered. The analytical dimensionless dispersion relation is derived for both axisymmetric and nonaxisymmetric perturbations and is solved for axisymmetric ones. Three unstable modes, i.e., the paravaricose, parasinuous and transitional modes, are identified in the Rayleigh regime. The influences of the axial electric field, liquid electrical properties, and Weber number are studied at length. The results show that the axial electric field has a generally stabilizing effect on the unstable modes. The effects of the liquid electrical properties are quite different but all great for each case. The change of dominant mode is detected with the variation of the electric field intensity, electrical properties or Weber number. It is found that the parasinuous instability is the easiest to realize in IDOC. And the comparison with the experiment validates that the parasinuous mode is predominant in coaxial electrospray.

DOI: 10.1103/PhysRevE.74.036304 PACS number(s): 47.20.−k, 47.65.−d, 47.15.Fe

I. INTRODUCTION

Liquid jets subjected to appropriate electric fields exhibit an amazing advantage in making micro/nanoparticles (electrospray) and ultrafine fibers (electrospinning). The most remarkable function of electric field is to help control production process easily and get ideal products. According to the orientation of electric field relative to liquid flow, there are usually two kinds of electric field, i.e., the axial and the radial, being used in various applications for different purposes. In general, the axial electric field stabilizes a jet and the radial destabilizes it.

Recently, an electrified coaxial jet with one liquid coated with the other was proposed [1] and proved to have an excellent ability in producing hollow or compound micro/nanoparticles (coaxial electrospray) and ultrathin fibers (coaxial electrospinning). Extensive experimental researches on the mechanism of generating compound droplets, the relevant scaling laws, and the feasibility of producing hollow or composite nanofibers have been carried out [1–7].

The behaviors of electrified coflowing jets are closely connected with the propagation and growth of disturbance waves on them. Amplified disturbance waves propagate downstream under the influence of surface tension and electrostatic force, making the jet break up ultimately. Therefore instability analysis is one of the most important subjects for jets. Up to now, most reports dealt with the axisymmetric instability of single liquid jets in electrospray [8–24]. The instability process occurring in electrospinning is essentially different from that in electrospray owing to its strongly nonaxisymmetric characteristic [25,26]. An electrically driven bending instability has been established [27,28]. By using a one-dimensional model [29,30], three unstable modes, i.e., the Rayleigh, axisymmetric conducting and whipping conducting modes, were identified.

Compared with single liquid jets, the behaviors of coflowing jets are much more complicated because two liquids with two interfaces (the inner liquid-liquid interface and the outer gas-liquid interface) are involved. In the axisymmetric instability analysis of a coflowing jet under a radial electric field [32], three unstable modes, i.e., the parasinuous, the paravaricose and the transitional mode, were identified in the Rayleigh regime. Obviously, coaxial electrospray is associated with the parasinuous instability [1–3]. As to coaxial electrospinning, it is probably associated with the first-order nonaxisymmetric mode in the early evolution process of jet instability [33].

The authors have studied the effect of a radial electric field on the axisymmetric instability of a coaxial inviscid jet [32,34,35]. The purpose of this paper is to study the effect of an axial electric field. The paper is organized as follows. In Sec. II, the theoretical model is described and the dispersion relation is given. In Sec. III, the unstable modes are calculated. The effects of the axial electric field, the interface tension and the electrical properties of the liquids on the jet instability are discussed. In Sec. IV, main conclusions are drawn.

II. THEORETICAL MODEL

Consider an infinitely long coflowing jet consisting of a cylindrical liquid jet of radius R_1 and an annular liquid jet of radius R_2 ($R_2 > R_1$) (as shown in Fig. 1). The ambient gas medium is maintained stationary in the unperturbed state. It is assumed that both the liquids and gas are incompressible and inviscid, having uniform density ρ_1 (the inner liquid), ρ_2 (the outer liquid), and ρ_3, respectively, and that the inner and outer liquids have uniform basic axial flow velocities U_1 and U_2, respectively. The whole system is subjected to a uniform electric field E_0 in the axial direction. The flow is irrotational. Those effects of gravity, magnetic field, and temperature are neglected. It is also assumed that there is no mass

*Electronic address: xzyin@ustc.edu.cn

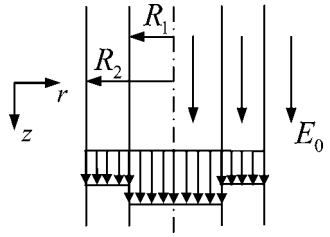

FIG. 1. Schematic description of a coflowing jet under a uniform axial electric field.

transfer across interfaces and that there is no source or sink of charge in bulks or on interfaces.

It is well known that for a conducting liquid the electrical relaxation time $T_e \sim \varepsilon_0 \varepsilon/\sigma$ (where ε_0, ε, and σ are the vacuum permittivity, the relative permittivity, and conductivity of liquid, respectively) is much smaller than the characteristic hydrodynamic time T_h, so that free charge is relaxed on the liquid surface almost instantaneously. For a perfectly dielectric liquid no free charge can be transported downstream unless the charge injection technique is used, which is beyond our research. In the present model, the surface charge density, if any, is assumed to be so low that the electric field due to surface charge is negligible compared with the axial electric field E_0.

The electrical property of a liquid plays an important role in coaxial electrospray. If the outer liquid is a conductor and the inner a dielectric, the electrical relaxation time of the outer liquid is much smaller than that of the inner and therefore charge is located on the outer gas-liquid interface. Conversely, if the inner liquid is a conductor and the outer a dielectric, the electrical relaxation time of the inner liquid is much smaller and charge lies on the inner liquid-liquid interface [2]. In the following theoretical analysis, four independent cases are taken into account according to the electrical properties of the inner and outer liquids. They are IDOC (inner: dielectric; outer: conductor), ICOD (inner: conductor; outer: dielectric), ICOC (inner and outer: conductor), and IDOD (inner and outer: dielectric). The electrical conductivity and permittivity of the liquids are assumed to be uniform and constant in all the cases.

For the flow the governing equations and boundary conditions used in the stability analysis are similar to those described in Ref. [34] [i.e., the continuity equation (1), the momentum equations (2) and (3), the kinematic boundary condition (7), and the dynamic boundary conditions (8) and (9) there]. Although the governing equation of electric field is the same as that in the case of the radial electric field [34], i.e., $\nabla^2 V_i = 0$, $i=1$, 2, and 3, where the subscripts 1, 2, and 3 stand for the inner liquid, the outer liquid and the ambient gas, respectively, and V_i is such a potential function that the electric field intensity $\mathbf{E}_i = -\nabla V_i$. The only thing that should be stressed is that the boundary conditions related to electric field, which must be used in derivation, are a little different in the four cases. Besides the continuity condition of the tangential electric fields, i.e., $\mathbf{n} \times \|\mathbf{E}\| = 0$, which should be satisfied on both the interfaces of all the cases, the continuity condition of the normal current densities, i.e., $\mathbf{n} \cdot \|\boldsymbol{\sigma}\mathbf{E}\| = 0$, is used on the interfaces having free charge, including the outer interface of IDOC, the inner interface of ICOD, and the outer interface of ICOC (the treatment of the inner interface of ICOC is delicate, and here we also choose this condition), and the Gauss' law, $\mathbf{n} \cdot \|\boldsymbol{\varepsilon}\mathbf{E}\| = 0$, is used on the other interfaces having no charge. Here, the symbol $\|^*\|$ is used to denote the jump of a quantity across the interface.

The perturbed velocity field, pressure, and electrical potential are all decomposed into the form of $(u,v,w,p,V)_i = (U+u', v', w', p_0+p', V_0+V')_i$, $i=1$, 2, and 3, where u, v, and w are the axial, radial and azimuthal velocity components, respectively. The subscript 0 and the prime denote the basic and perturbation parts of the corresponding quanti-

TABLE I. Expressions of the symbols in the dispersion relation for the four cases.

Cases	h_1	h_2	h_3	h_4	T
IDOC	$\left(\frac{\varepsilon_{p2}}{\varepsilon_{p1}}-1\right)\frac{\Delta_4}{T}$	$\frac{\varepsilon_{p2}\Delta_1}{\varepsilon_{p1}T}$	$\frac{I_n'(\alpha a)\Delta_2 - \frac{\varepsilon_{p2}}{\varepsilon_{p1}} I_n(\alpha a)\Delta_3}{T}$	$\left(\frac{\varepsilon_{p2}}{\varepsilon_{p1}}-1\right)$	a
ICOD	$\frac{1}{I_n'(\alpha a)}$	0	$(\varepsilon_{p2}-1) I_n'(\alpha a) K_n(\alpha) \frac{\Delta_2}{T}$	$\varepsilon_{p2} K_n(\alpha)$	b
ICOC	$\left(\frac{1}{\sigma_r}-1\right)\frac{\Delta_4}{T}$	$\frac{\Delta_1}{\sigma_r T}$	$\frac{I_n'(\alpha a)\Delta_2 - \frac{1}{\sigma_r} I_n(\alpha a)\Delta_3}{T}$	$\left(\frac{1}{\sigma_r}-1\right)$	c
IDOD	$\frac{\left(\frac{\varepsilon_{p2}}{\varepsilon_{p1}}-1\right)[\varepsilon_{p2} K_n(\alpha)\Delta_4 - K_n'(\alpha)\Delta_2]}{T}$	$\frac{\frac{\varepsilon_{p2}}{\varepsilon_{p1}}(\varepsilon_{p2}-1) K_n(\alpha)\Delta_1}{T}$	$K_n(\alpha)(\varepsilon_{p2}-1)\frac{\frac{\varepsilon_{p2}}{\varepsilon_{p1}} I_n(\alpha a)\Delta_3 - I'_n(\alpha a)\Delta_2}{T}$	$\varepsilon_{p2}\left(\frac{\varepsilon_{p2}}{\varepsilon_{p1}}-1\right) K_n(\alpha)$	d

a: $[I_n'(\alpha a) K_n(\alpha a) - \varepsilon_{p2}/\varepsilon_{p1} I_n(\alpha a) K_n'(\alpha a)] I_n'(\alpha) + I_n(\alpha a) I_n'(\alpha a) K_n'(\alpha)(\varepsilon_{p2}/\varepsilon_{p1}-1)$,
b: $[I_n(\alpha) K_n'(\alpha) - \varepsilon_{p2} I_n'(\alpha) K_n(\alpha)] I_n'(\alpha a) K_n(\alpha a) + I_n(\alpha a) I_n'(\alpha a) K_n(\alpha) K_n'(\alpha)(\varepsilon_{p2}-1)$,
c: $[I_n'(\alpha a) K_n(\alpha a) - 1/\sigma_r I_n(\alpha a) K_n'(\alpha a)] I_n'(\alpha) + I_n(\alpha a) I_n'(\alpha a) K_n'(\alpha)(1/\sigma_r - 1)$,
d: $I_n(\alpha a) I_n'(\alpha a) K_n(\alpha) K_n'(\alpha)(\varepsilon_{p2}/\varepsilon_{p1}-1)(\varepsilon_{p2}-1) - [I_n(\alpha) K_n'(\alpha) - \varepsilon_{p2} I'_n(\alpha) K_n(\alpha)][I_n'(\alpha a) K_n(\alpha a) - \varepsilon_{p2}/\varepsilon_{p1} I_n(\alpha a) K'_n(\alpha a)]$.

ties, respectively. The interfaces being perturbed are $r_{sj}=R_j+\eta_j$, $j=1$ and 2, where η_j is the displacement of the interface from their original radius R_j, and the subscripts 1 and 2 denote the inner liquid-liquid and outer gas-liquid interfaces, respectively. Then the classical process of the normal modal method is implemented straightforwardly. The perturbations of the velocity, pressure, electrical potential and interface are all decomposed into the form of a Fourier exponential, i.e., $(\mathbf{u}',p',V')_i=[\hat{\mathbf{u}}(r),\hat{p}(r),\hat{V}(r)]_i e^{\omega t+i(kz+n\theta)}$, $i=1$, 2, and 3, and $\eta_j=\eta_{0j}e^{\omega t+i(kx+n\theta)}$, $j=1$ and 2, with $\hat{\mathbf{u}}(r)$, $\hat{p}(r)$, and $\hat{V}(r)$ the amplitudes of the corresponding quantities, η_0 the initial disturbance amplitude on the interface, k and n the axial and azimuthal wave numbers, respectively, and ω the complex frequency.

After straightforward calculation, the dispersion relation can be obtained. It is written in the dimensionless form as follows:

$$D(\alpha,\beta)=\frac{H_1\Delta_5+\Delta_4}{H_2\Delta_5+\Delta_1}+\frac{H_4\Delta_5-\Delta_6}{H_3\Delta_5-\Delta_3}=0, \tag{1}$$

with

$$H_1=\frac{-S(\beta+i\Lambda\alpha)^2\dfrac{I_n(\alpha a)}{I_n'(\alpha a)}+\dfrac{\Gamma\alpha}{\mathrm{We}\alpha^2}[1-n^2-(\alpha a)^2]+\alpha^2 E I_n(\alpha a)(\varepsilon_{p2}-\varepsilon_{p1})h_1}{(\beta+i\alpha)^2},$$

$$H_2=\frac{\alpha^2 E I_n(\alpha a)(\varepsilon_{p2}-\varepsilon_{p1})h_2}{(\beta+i\alpha)^2},$$

$$H_3=\frac{Q\beta^2\dfrac{K_n(\alpha)}{K_n'(\alpha)}+\dfrac{\alpha}{\mathrm{We}}(1-n^2-\alpha^2)+\alpha^2 E(\varepsilon_{p2}-1)h_3}{(\beta+i\alpha)^2},$$

$$H_4=-\frac{\alpha^2 E(\varepsilon_{p2}-1)}{(\beta+i\alpha)^2}\cdot\frac{I_n(\alpha a)\Delta_6 h_4}{T}.$$

The expressions of h_1-h_4 for the four cases are given in Table I. And $\Delta_1-\Delta_6$ are

$$\Delta_1=I_n(\alpha a)K_n'(\alpha a)-I_n'(\alpha a)K_n(\alpha a),\quad \Delta_2=I_n(\alpha a)K_n(\alpha)-I_n(\alpha)K_n(\alpha a),$$

$$\Delta_3=I_n'(\alpha a)K_n(\alpha)-I_n(\alpha)K_n'(\alpha a),\quad \Delta_4=I_n(\alpha a)K_n'(\alpha)-I_n'(\alpha)K_n(\alpha a),$$

$$\Delta_5=I_n'(\alpha a)K_n'(\alpha)-I_n'(\alpha)K_n'(\alpha a),\quad \Delta_6=I_n(\alpha)K_n'(\alpha)-I_n'(\alpha)K_n(\alpha),$$

where $I_n(x)$ and $K_n(x)$ are the nth-order modified Bessel functions of the first and second kinds, respectively, and the prime denotes the derivative with respect to x.

Here α and β are the dimensionless wave number and frequency, respectively, which are normalized by $1/R_2$ and U_2/R_2. The dimensionless parameters involved include the density ratios $S=\rho_1/\rho_2$ and $Q=\rho_3/\rho_2$, the velocity ratio $\Lambda=U_1/U_2$, the diameter ratio $a=R_1/R_2$, the interfacial tension coefficient ratio $\Gamma=\gamma_1/\gamma_2$, the relative electrical permittivities $\varepsilon_{p1}=\varepsilon_1/\varepsilon_3$ and $\varepsilon_{p2}=\varepsilon_2/\varepsilon_3$, the conductivity ratio $\sigma_r=\sigma_1/\sigma_2$, the Weber number $\mathrm{We}=\rho_2U_2^2R_2/\gamma_2$, and the dimensionless electrostatic force $E=\varepsilon_3E_0^2/\rho_2U_2^2$. Compare with the results in Refs. [32,34], it can be found that the dispersion relation here is more complicated, predicting that the effects of the axial electric field on the jet instability are more difficult to analyze than the case of the radial electric field.

The dispersion relation (1) can be reduced to that of the single liquid jet subjected to a uniform axial electric field. For example, in IDOC, if the radius of the inner liquid jet approaches zero (i.e., $R_1\to 0$), the coaxial jet turns into a jet of a conducting liquid. Note that under this condition both $K_n(kR_1)$ and $K_n'(kR_1)$ approach infinity. The corresponding dispersion relation written in the dimensional form is

$$\rho_3\omega^2\frac{K_n(kR_2)}{K_n'(kR_2)}+\frac{\gamma_2 k}{R_2^2}[1-n^2-(kR_2)^2]-\frac{I_n(kR_2)}{I_n'(kR_2)}[\rho_2(\omega+ikU_2)^2+k^2E_0^2(\varepsilon_2-\varepsilon_3)]=0. \tag{2}$$

In ICOD, if $R_1\to 0$, the coaxial jet becomes a jet of a dielectric liquid, resulting in the following dispersion relation

TABLE II. Values of the dimensionless parameters in the reference state.

Cases	S	Q	a	Λ	We	Γ	ε_{p1}	ε_{p2}	σ_r
IDOC	0.84	0.001	0.8	0.8	10	0.23	3.4	80	/
ICOD	1.19	0.001	0.8	1.25	10	0.51	80	3.4	/
ICOC	0.8	0.001	0.8	0.8	10	0.40	10	10	0.8
IDOD	0.8	0.001	0.8	0.8	10	0.40	10	10	/

$$\rho_3\omega^2\frac{K_n(kR_2)}{K_n'(kR_2)}+\frac{\gamma_2 k}{R_2^2}[1-n^2-(kR_2)^2]-\rho_2(\omega+ikU_2)^2\frac{I_n(kR_2)}{I_n'(kR_2)}$$
$$+k^2E_0^2(\varepsilon_2-\varepsilon_3)\frac{\left(\frac{\varepsilon_2}{\varepsilon_3}-1\right)I_n(kR_2)K_n(kR_2)}{I_n(kR_2)K_n'(kR_2)-\frac{\varepsilon_2}{\varepsilon_3}I_n'(kR_2)K_n(kR_2)}=0. \tag{3}$$

Zakaria [21] and Othman [36] obtained the same dispersion equations in their stability researches of single liquid jets, respectively.

III. NUMERICAL RESULTS AND DISCUSSION

In order to have an insight into the axisymmetric instability behaviors of the coflowing jet under a uniform axial electric field, the dispersion relation (1) is solved numerically. We use the typical data in experiments, for example, water is chosen as the outer liquid and sunflower oil as the inner liquid for IDOC (their physical properties can be found in Ref. [2]). The values of the Weber number and dimensionless electrostatic force are estimated at 10 and 0.0001, respectively [3,34]. The values of the other dimensionless parameters chosen as references are shown in Table II for the four cases. For convenience of comparison, in the following calculations these parameters are fixed as a reference state except clarified otherwise.

A. Unstable modes and effect of the axial electric field

Similar to the instability analysis of the coaxial jet under a radial electric field [32], the calculation results show that in the case of the axial electric field there generally exist three unstable modes according to the phase difference of initial disturbances at the inner and outer interfaces. They are the paravaricose mode (out of phase), the parasinuous mode (in phase), and the transitional mode (changing continuously from in phase to out of phase). In most situations, the parasinuous and transitional modes are combined together. Figures 2(a)–2(f) illustrates the effect of the axial electric field on the growth rate β_r of the unstable modes for IDOC, ICOD, and ICOC, respectively (IDOD is not plotted because it is very similar to ICOC). In Fig. 2, the left column corresponds to the paravaricose mode, the left peaks in the right column correspond to the parasinuous mode, and the right to the transitional mode.

Completely different from the destabilizing effect of the radial electric field [32], it can be seen from the figures that the axial electric field has a stabilizing effect on the unstable modes, no matter for which case. But the details are quite different in these cases. For IDOC, the growth rates of the paravaricose and transitional modes are suppressed by the electric field much more evidently than that of the parasinuous mode. When the dimensionless electrical force E reaches 0.0005, the paravaricose and transitional modes vanish, whereas the parasinuous mode is almost unchanged. When E is larger than 0.0005, the parasinuous mode begins to be stabilized visibly but slowly. Hence, the parasinuous mode is always the most unstable, and dominates the jet instability in IDOC. However, for ICOD the electric field has a remarkably stabilizing effect on the parasinuous and transitional modes. When E is 0.001, these two modes vanish, but the paravaricose mode is affected greatly only if the electric field is sufficiently large. Obviously, the paravaricose mode may be predominant in this case, provided that the axial electric field intensity is large enough. As is well known [31], the parasinuous and paravaricose modes are associated mainly with the inner and outer interfaces, respectively. According to our result that in IDOC the paravaricose mode is sensitive to the electric field but in ICOD the parasinuous mode does,

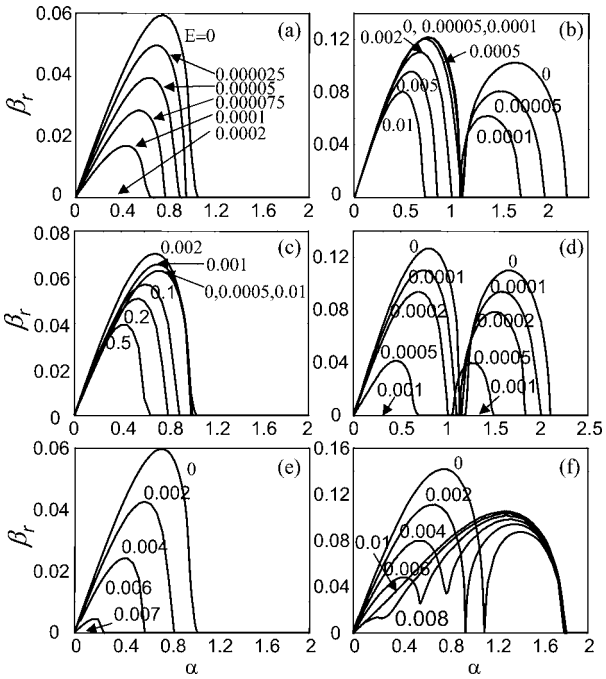

FIG. 2. Influence of the dimensionless electrostatic force E on the growth rate β_r of the paravaricose mode (left column) and the parasinuous and transitional modes (right column) for (a,b) IDOC, (c,d) ICOD, and (e,f) ICOC.

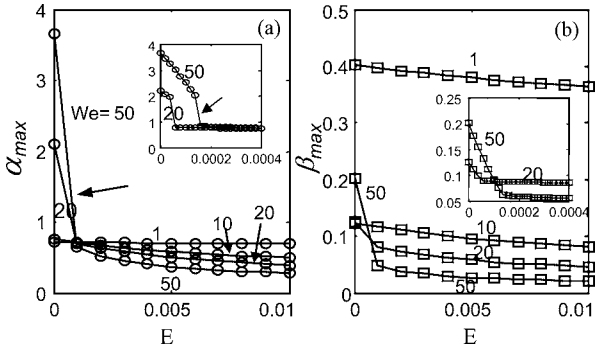

FIG. 3. (a) The dominant axial number α_{max} and (b) maximum growth rate β_{max} for IDOC versus the dimensionless electrostatic force E under different values of the Weber number We.

it comes to the conclusion that the axial electric field influences the unstable mode related to the outer surface of the conducting liquid much more strongly than that related to the outer surface of the dielectric liquid.

ICOC and IDOD is another case. For them, the growth rates of both the paravaricose and the parasinuous mode are diminished distinctly, while that of the transitional mode is amplified visibly by the axial electric field. We attribute these different behaviors of the unstable modes under the electric field to the difference of the electrical property of liquid in the four cases. On the other hand, the effect of the electric field on the unstable wave number range is quite similar to its effect on the growth rates in the four cases.

B. Dominant mode due to the surface/interface tensions

In our model, the dimensionless parameters relevant to surface/interface tensions are the Weber number We and the interfacial tension coefficient ratio Γ. According to the previous studies [31,34], the interfacial tension coefficient ratio Γ behaves in a similar way with the Weber number in jet instability. Therefore we only investigate the influence of Weber number in the following. For the sake of a more general view, a relatively wide range of Weber number (i.e., $1 < \mathrm{We} < 50$) is calculated.

When arbitrary disturbances are enforced on a jet, the wave having maximum growth rate and those close to it grow faster than the others and dominate in the breakup process of the jet ultimately. In Fig. 2 it is shown that the axial electric field diminishes the dominant axial wave number generally. Now we will investigate the effect of the Weber number together with the axial electric field on the dominant wave number α_{max} and corresponding maximum growth rate β_{max}. Taking IDOC as an example (as shown in Fig. 3), it is notable that at relatively large Weber numbers and relatively small dimensionless electrostatic forces the transitional mode is dominant (the characteristic of the transitional mode is that its corresponding dominant wave number is larger than one). But with the electric field increasing, the dominant mode turns into the parasinuous one (the position of the "mode shift" is marked with arrows in the figure). On the other hand, when the transitional mode is dominant, the dominant wave number is augmented by the Weber number, whereas

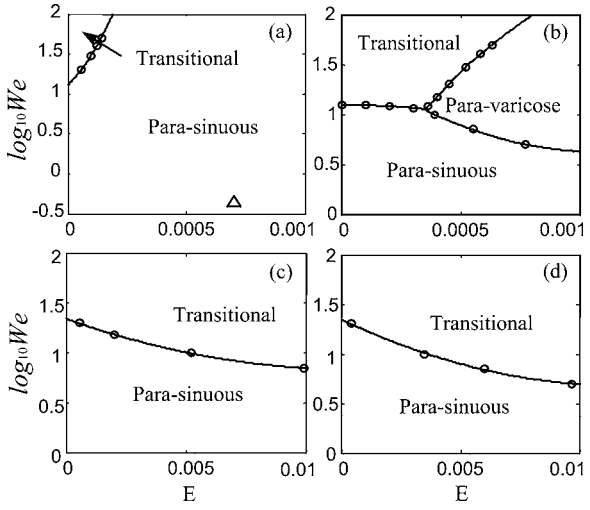

FIG. 4. Boundary curves on the We-E plane for (a) IDOC, (b) ICOD, (c) ICOC, and (d) IDOD.

when the parasinuous mode becomes dominant, the Weber number can reduce α_{max} slightly. And the maximum growth rate is generally diminished by the Weber number. It is obvious that at different We's the maximum growth rate is always stabilized by the axial electric field.

In order to illuminate the influence of We and E on the shift of dominant mode further, Figs. 4(a)–4(d) represents the fitting curves of the boundary between dominant modes for the four cases, respectively, on the We-E plane. For a wide range of We and E in IDOC [as shown in Fig. 4(a)], the parasinuous mode is predominant except in a small region with large We's and small E's where the transitional mode is dominant. In ICOD, three boundary lines are found, which divide the plane into three parts [Fig. 4(b)]. When E is smaller than a critical value ($\sim$0.000 35), the parasinuous mode dominates the region where $\mathrm{We} < 12$, and the transitional mode dominates where $\mathrm{We} > 12$. When E exceeds the critical value, the dominant mode is the parasinuous, paravaricose, and transitional modes successively with We increasing. Both ICOC [Fig. 4(c)] and IDOD [Fig. 4(d)] have only one boundary line. The dominant regions of the parasinuous mode and the transitional mode appear below and above it, respectively. Figure 4 reminds us that the magnitudes of We and E must be treated carefully. In general, it seems easier to realize coaxial electrospray in IDOC, which is the very case that most experiments dealt with successfully. For the other three cases, our result shows that it is better to keep We and E relatively small.

C. Dominant wave number due to the electric field and liquid electrical properties

In this section, we discuss briefly the importance of the electrical property of liquid in coaxial electrospray through their effects on the dominant wave number and maximum growth rate. Taking IDOC and ICOD as examples, the influences of the relative electrical permittivities ε_{p1} and ε_{p2} on the dominant wave number α_{max} and maximum growth rate β_{max} are illustrated in Figs. 5 and 6, respectively. It can be

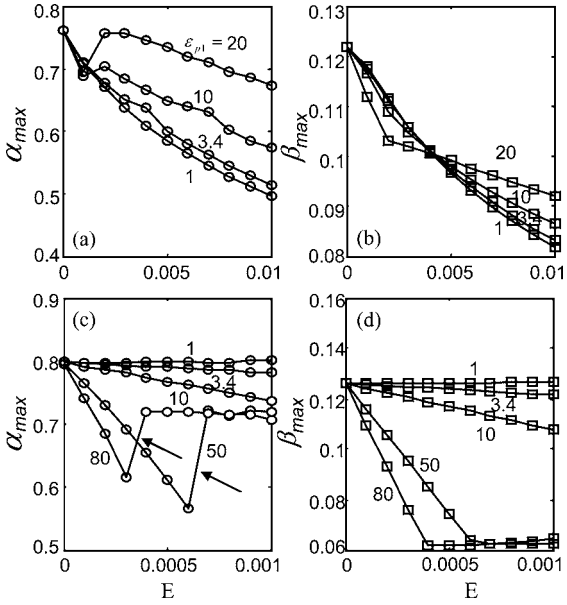

FIG. 5. The dominant axial number α_{max} and maximum growth rate β_{max} for (a,b) IDOC and (c,d) ICOD versus the dimensionless electrostatic force E under different values of the relative electrical permittivity ε_{p1}.

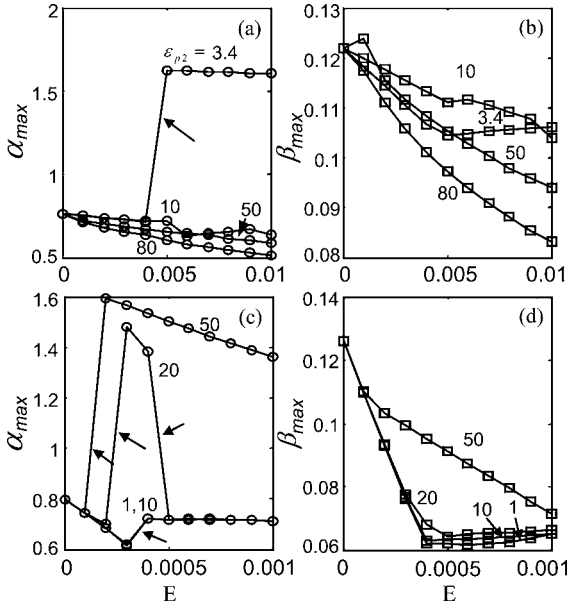

FIG. 6. The dominant axial number α_{max} and maximum growth rate β_{max} for (a-b) IDOC and (c,d) ICOD versus the dimensionless electrostatic force E under different values of the relative electrical permittivity ε_{p2}.

seen that in both the cases the electrical permittivities of the inner and outer liquids have obvious effects on the magnitudes of α_{max} and β_{max}. Moreover, the dominant mode may be changed by the relative electrical permittivities with the help of the axial electric field. In general, the parasinuous mode is predominant when the electric field is relatively small, regardless of the permittivity and conductivity of liquid. In addition, the dominant wave number and corresponding growth rate are decreased more or less by the electric field. However, as the electric field intensity is amplified sufficiently, the "mode shift" may be induced, and the electrical properties of the liquids influence this shift greatly. For example, larger ε_{p1} accelerates the shift of dominant mode from the parasinuous into the paravaricose in ICOD, and ε_{p2} makes the dominant mode change into the transitional at relatively large values while into the paravaricose at relatively small values. Unfortunately, it is difficult to figure out clearly the effects of liquid electrical permittivity and conductivity in the four cases, so we cannot give a general picture of them for the moment. And it seems better that every case is analyzed specially.

D. Comparison with the experimental results

In coaxial electrospray experiments, the typical diameter of coaxial liquid jets is approximately of the order of ten micrometers. For such a thin jet, effect of liquid viscosity is of remarkable significance. That is, liquid viscosity plays an important role in jet instability, not only influencing basic velocity profile but also providing viscous shearing force to balance tangential electrical stress on the interface. Our inviscid model is a simplified one. But, in this paper we aim to get an analytical dispersion relation and a primary understanding about the behaviors of the axial electric field. The inviscid model does help in a sense.

As to the basic velocity profile, besides the uniform one assumed in this inviscid model, Mestel [10] and Turnbull [13,14] both used a more realistic parabolic radial velocity profile, taking account of the influence of electrical shear stress, in their instability analysis of a single liquid jet under electric field. López-Herrera *et al.* [18] discussed briefly the effect of the Ohnesorge number that weighs viscous force against capillary force on the radial profile of axial velocity.

In spite of all these assumptions, we simply compare our numerical result with the experiment [3]. In Chen's coaxial electrospray with an outer driving liquid (i.e., IDOC), the inner liquid is cooking oil and the outer liquid a mixture of ethanol, glycerol, and tween. Their physical properties and experiment conditions can be found in Refs. [2,3]. The corresponding dimensionless parameters are as follows: $S=0.95$, $Q=0.001$, $n=0$, $a=0.77$, $\Lambda=1$, $\Gamma=0.12$, We$=0.44$, $E=7\times10^{-4}$, $\varepsilon_{p1}=3.4$, and $\varepsilon_{p2}=41$. The location of the experiment state is plotted on the We-E plane [the triangle marker in Fig. 4(a)]. It lies in the dominant region of the parasinuous mode, indicating that the parasinuous mode is predominant, which is accordant with the experiment qualitatively. Noting that the value of the dimensionless electrostatic force is considerably small, the effect of electric field is limited. However, it should be mentioned that the electric field in experiments may be very complex and the above value is just an approximate one.

IV. CONCLUSION

In this paper, we have studied the instability of a coflowing cylindrical jet subjected to a uniform axial electric field

using a simple inviscid model. According to the electrical properties of the inner and outer liquids, four different cases, i.e., IDOC, ICOD, ICOC, and IDOD, are considered. The dimensionless dispersion relation is derived analytically for all these cases and the eigenfrequency is solved numerically. Three unstable modes, i.e., the paravaricose, parasinuous, and transitional modes, are identified in the Rayleigh regime.

The axial electric field is found to have a stabilizing effect on the unstable modes except that it destabilizes the transitional mode a little in ICOC and IDOD. The numerical result shows that the parasinuous mode, the paravaricose mode, and the transitional mode are influenced the least by the axial electric field in IDOC, ICOD, and ICOC (or IDOD), respectively, and accordingly may dominate in the corresponding cases. The electrical property of liquid proves to play an important role in jet instability. They not only result in four different cases with different dispersion relations but influence the instability details of each case. The effects of the electric field and electrical properties on the dominant wave number and maximum growth rate are studied for each case. Though their effects are various, the axial electric field and the electrical properties of the liquids influence the jet instability significantly. In particular, they can induce the change of dominant mode. The Weber number also has a great effect on the instability of jet. The dominant regions of the unstable modes are distinguished on the We-E plane. It is shown that in IDOC the parasinuous mode occupies most of the region on the parameter plane. And therefore coaxial electrospray is relatively easy to realize in this case.

ACKNOWLEDGMENTS

This work was supported by the National Natural Science Foundation of China Project No. 10572137 and the Graduate Innovation Project of USTC No. KD2005036.

[1] G. Loscertales, A. Barrero, I. Guerrero, R. Cortijo, M. Márquez, and A. M. Gañán-Calvo, Science **95**, 1695 (2002).
[2] J. M. López-Herrera, A. Barrero, A. López, I. G. Loscertales, and M. Márquez, J. Aerosol Sci. **34**, 535 (2003).
[3] X. P. Chen, L. B. Jia, X. Z. Yin, J. S. Cheng, and J. Lu, Phys. Fluids **17**, 032101 (2005).
[4] Z. C. Sun, E. Zussman, A. L. Yarin, J. H. Wendorff, and A. Greiner, Adv. Mater. (Weinheim, Ger.) **15**, 1929 (2003).
[5] D. Li and Y. Xia, Nano Lett. **4**, 933 (2004).
[6] J. H. Yu, S. V. Fridrikh, and G. C. Rutledge, Adv. Mater. (Weinheim, Ger.) **16**, 1562 (2004).
[7] D. Li, J. T. Mccann, and Y. Xia, Small **1**(1), 83 (2005).
[8] A. M. Gañán-Calvo, J. C. Lasheras, J. Dávila, and A. Barrero, J. Aerosol Sci. **25**, 1121 (1994).
[9] A. M. Gañán-Calvo, J. Dávila, and A. Barrero, J. Aerosol Sci. **28**(2), 249 (1997).
[10] A. J. Mestel, J. Fluid Mech. **274**, 93 (1994).
[11] D. A. Saville, Phys. Fluids **13**, 2987 (1970).
[12] D. A. Saville, Phys. Fluids **14**, 1095 (1971).
[13] R. J. Turnbull, IEEE Trans. Ind. Appl. **28**(6), 1432 (1992).
[14] R. J. Turnbull, IEEE Trans. Ind. Appl. **32**(4), 837 (1996).
[15] G. Artana, H. Romat, and G. Touchard, J. Electrost. **43**, 83 (1998).
[16] F. J. García, H. González, A. Ramos, and A. Castellanos, J. Electrost. **40&41,** 161 (1997).
[17] H. González, F. J. García, and A. Castellanos, Phys. Fluids **15**(2), 395 (2003).
[18] J. M. López-Herrera, P. Riesco-Chueca and A. M. Gañán-Calvo, Phys. Fluids **17**, 034106 (2005).
[19] J. M. López-Herrera, A. M. Gañán-Calvo, and M. Perez-Saborid, J. Aerosol Sci. **30**, 895 (1999).
[20] J. M. López-Herrera and A. M. Gañán-Calvo, J. Fluid Mech. **501**, 303 (2004).
[21] K. Zakaria, Fluid Dyn. Res. **26**, 405 (2000).
[22] A. R. F. Elhernawy, B. M. H. Agoor, and A. E. K. Elcoot, Physica A **297**, 368 (2001).
[23] A. R. F. Elhernawy, G. M. Moatimid, and A. E. K. Elcoot, ZAMP **55**, 63 (2004).
[24] G. M. Moatimid, J. Phys. A **36**, 11343 (2003).
[25] Y. M. Shin, M. M. Holman, M. P. Brenner, and G. C. Rutledge, Appl. Phys. Lett. **78**, 1149 (2001).
[26] Y. M. Shin, M. M. Holman, M. P. Brenner, and G. C. Rutledge, Polymer **42**, 9955 (2001).
[27] D. H. Reneker, A. L. Yarin, H. Fong, and S. Koombhongse, J. Appl. Phys. **87**, 4531 (2000).
[28] A. L. Yarin, S. Koombhongse, and D. H. Reneker, J. Appl. Phys. **89**, 3018 (2001).
[29] M. M. Hohman, M. Shin, G. Rutledge, and M. P. Brenner, Phys. Fluids **13**, 2201 (2001).
[30] M. M. Hohman, M. Shin, G. Rutledge, and M. P. Brenner, Phys. Fluids **13**, 2221 (2001).
[31] J. Shen and X. Li, Acta Mech. **114**, 167 (1996).
[32] F. Li, X. Y. Yin, and X. Z. Yin, Phys. Fluids **18**, 037101 (2006).
[33] P. H. Son and K. Ohba, Int. J. Multiphase Flow **24**, 605 (1998).
[34] F. Li, X. Y. Yin, and X. Z. Yin, Phys. Fluids **17**, 077104 (2005).
[35] F. Li, X. Y. Yin, and X. Z. Yin, J. Electrost. **64**, 690 (2006).
[36] M. I. A. Othman, ZAMP **49**, 759 (1998).